Living With a Star TR&T Program: NNH05ZDA001N

Annual Report: First Year Progress Report and Second Year Goals

Tracking Photospheric Magnetic Footpoints with the Magnetic Induction Equation

PI: Peter W. Schuck, Co-I's: Jonathon Krall and Joseph D. Huba
Naval Research Laboratory, Washington, DC, 20375-5346

NASA OSS LWS TR&T-NNH05ZDA001N is a three-year program to develop techniques for accurate and precise estimation of solar surface flows from magnetogram data. Local Correlation Tracking (LCT) is the de-facto standard for estimating motion in solar image sequences. However, this technique has many documented limitations. Perhaps the greatest limitations of LCT are the absence of demonstrated accuracy, precision and a quantifiable local uncertainty associated with the velocities derived from this technique, and the introduction of artificial scales. This *program has already developed new techniques* that are less susceptible to these limitations (Schuck, 2006; Welsch et al., 2007). The technique called the differential affine velocity estimator (DAVE) determines the optical flow by applying the magnetic induction equation and an affine velocity model statistically to a windowed subregion of the magnetogram sequence producing an overdetermined system that can be solved directly by standard least squares or total least squares techniques. These subspace methods are inherently statistical. Consequently, the optical flow estimates can be assessed for reliability and for resolution of the aperture problem. The result is a point-by-point optical flow field that is consistent with the magnetic induction equation. The new algorithms have been benchmarked against synthetic data and high-β MHD simulations to establish the accuracy of the technique and compared against the accuracy of previously developed optical flow techniques such as LCT, Inductive Local Correlation Tracking (ILCT), and Minimum Energy Fit (MEF).

Work Statement and Important Milestones

The program incorporates two components. The first component involves algorithm and code development, the extension of the established method to implement all components of vector magnetogram data, tools for computing helicity and magnetic energy flux from the optical flow and magnetogram data, and tools for benchmarking optical flow algorithms against synthetic data. The second component of the program supports the solar physics community by providing *standardized* test data for future optical flow techniques and by identifying and acquiring solar data for events that the solar physics community will incorporate into MHD simulations (Fisher & Solar MURI Team, 2003; Riley et al., 2001; Gudiksen & Nordlund, 2002; Roussev et al., 2003; Welsch et al., 2004; Longcope, 2004). The primary focus of the first and second years are on the first component.

A prime measure of success for this is the widespread use of these "tools" for the determination of solar surface flows from observational data and use of the standardized test data produced as a consequence of the program. The DAVE has already been implemented successfully by Chae et al. (2006). The algorithms and data sets have been/will be documented through peer-reviewed journal articles (Schuck, 2006; Welsch et al., 2007). More importantly, the library of tools and data sets developed under the program will be available to the solar physics community through IDL. We are presently in discussions with Sam Freeland to incorporate DAVE into the SolarSoft system.[1]

[1] `http://sohowww.nascom.nasa.gov/solarsoft/`

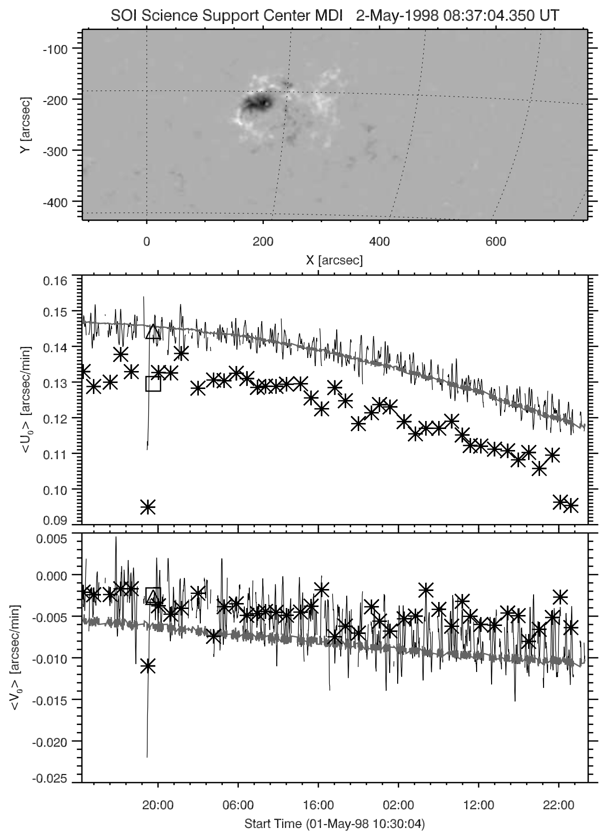

Figure 1: Line-of-Sight *SOHO*/MDI magnetogram of AR8210. (middle/bottom) The $\widehat{\boldsymbol{x}}$ and $\widehat{\boldsymbol{y}}$-components of the mean image active region velocity (arcsec/min). The noisy black line corresponds to the values computed from the DAVE and the isolated data points denoted by "($*$)" were determined by LCT. The thick continuous lines are the empirical values computed from Howard et al. (1990) and projected onto the image plane.

The time-table the important first and second year milestones us presented in detail below:

YEAR 1

A. *Develop tool for accurately evolving B_n in a prescribed flow and benchmark **DAVE** against this tool.*
Progress: Methods for generating synthetic test images are extensively documented in Section 5 of Schuck (2006). Several error metrics are developed and used to compare the performance of DAVE and LCT. These basic test codes will be incorporated into the SolarSoft release of DAVE.

As a demonstration of the method's capabilities, the DAVE was applied to approximately 2600 *SOHO*/MDI line-of-sight (LOS) magnetograms with a 1 minute cadence covering NOAA Active Region 8210 from 1998 May 1 when AR8210 was near disk center to 1998 May 4, when AR8210 was just inside of 60° W (See Scherrer et al., 1995, for a description of the *SOHO*/MDI instrument). During this time, AR8210, associated with a δ-sunspot, erupted with two M-class flares and one X-class flare concomitant with a Halo CME (Warmuth et al., 2000; Sterling & Moore, 2001; Sterling et al., 2001; Pohjolainen et al., 2001; Huang & Falthammar, 2002; Xia et al., 2002). This active region has been test bed for other magnetic feature tracking methods (Welsch et al., 2004; Longcope, 2004; Georgoulis & LaBonte, 2006). The top panel in Figure 1 shows a LOS *SOHO*/MDI magnetogram of AR8210. The magnetic footpoint velocities were computed for the entire time-period within the field of view using the DAVE. An 11×11 pixel top-hat window was used to localize the analysis combined with second order temporal differences and time-centered 5-point spatial differences. Each frame corresponded to an 11 minute temporal average of the 1-minute cadence MDI data images to reduce shot noise.

In contrast to other studies, the magnetogram data were not de-rotated prior to analysis; thus the estimated velocities correspond to the total velocity of the active region including synodic differential solar rotation as observed from MDI. This permits a fundamental test of the DAVE's reliability against an empirical differential rotation formula

$$R = A + B\,\sin^2\phi + C\,\sin^4\phi, \tag{1}$$

as a function of heliographic latitude ϕ, where R is the differential rotation rate in μrad/s and the constants $A = 2.894 \pm 0.011$, $B = -0.428 \pm 0.070$ and $C = -0.370 \pm 0.077$ have been determined by following magnetic tracers on the solar surface by a correlation tracking technique similar to LCT (Howard et al., 1990) (Also see the original work by Ward, 1965). Modern measurements of these constants, including spectroscopic ones, agree to within 5% (Beck, 2000).

The middle and bottom panels of Figure 1 show the $\widehat{\boldsymbol{x}}$ and $\widehat{\boldsymbol{y}}$-components of the mean active region magnetic footpoint velocity in the image plane (arcsec/min) determined from pixels where the median magnitude of the magnetic field exceeded 60 Gauss within the 11×11 apodizing window. The noisy black line corresponds to the values computed from the DAVE and the isolated data points denoted by "($*$)" were determined by LCT. While the dynamics of magnetic footpoints is not simply determined by the plasma velocity, the average motion of the magnetic footpoints should correspond favorably with other measurements of magnetic feature motion. The expected mean velocities were computed by mapping the image pixels corresponding to the active region onto the solar surface. The expected velocity of these magnetic elements was computed from equation (1) and these velocities were then projected back into the image plane while accounting for the curvature of the solar surface and the synodic motion of the satellite which decreases the observed rate of rotation by by $0.199\,\mu$rad/s. The thick continuous lines, corresponding to these expected values, agree favorably with the mean active region image velocity estimated for these same pixels by the DAVE. This indicates that the DAVE accurately captures the mean dynamics of the active region on large spatial scales. Notice how the $\widehat{\boldsymbol{x}}$ component of the apparent image velocity for AR8210 decreases predictably with time as the active region moves towards the west limb. Similarly, the trend in the $\widehat{\boldsymbol{y}}$ component of the image velocity becomes more negative due to the tilt of the sun's axis (P-angle) away from the earth at this time. There is a discernable bias to the mean $\langle V_0 \rangle$ values away from the empirical values and towards zero. This may be an indication of fundamental accuracy limits, an error in the P-angle (the estimated range for the B_0 angle during the corresponding time period was $B_0 = -4.06 \pm 0.08°$), or true equatorward motion of the active region at 25 m/s (c.f., Javaraiah, 1999). The agreement between the isolated LCT values and the empirical differential rotation formula is not as satisfactory. The mean $\widehat{\boldsymbol{x}}$ component of the LCT velocity is less than the empirical values by as much as 12% indicating an apparent subrotation of the active region. While the possibility exists that the active region is subrotating, this seems improbable and is perhaps indication of the accuracy limitations of LCT on the 8 minute timescale with an aperture size of $\sigma = 10$ pixels. Interestingly, the $\widehat{\boldsymbol{y}}$ component of the LCT velocities agrees favorably with the DAVE results perhaps indicating inherent accuracy limitations of both methods.

Figure 2 shows magnetic footpoint velocity field for AR8210 at 19:24 UT on 1998 May 1 determined from the DAVE (left) and LCT (right). Velocity vectors on positive footpoints are colored black and velocity vectors on negative footpoints are colored white. Time derivatives for DAVE were computed with a frame separation of $\Delta t = 8$ min. LCT was carried out with a frame separation of $\Delta t = 8$ min (top right) and $\Delta t = 4$ hours and 16 min (bottom right). The DAVE shows significantly more structure and detected clockwise rotation of the sunspot in agreement with Warmuth et al. (2000).

B. *Produce flux codes for computing the magnetic energy and helicity fluxes from* $\boldsymbol{B}$ *and* $\boldsymbol{u}_{\mathrm{F}}$ *(the footpoint velocity).*

Progress: A IDL code implementing MUDPACK[2] has been developed to estimate the helicity flux by enforcing Dirichlet boundary conditions on ψ of the vector potential $\mathbf{A} = \widehat{\mathbf{n}} \times \nabla\psi$. The computations are performed in spherical coordinates transformed into the image plane which accounts for the curvature of the solar surface in the image plane. The results for AR8210 are shown in Figure 3.

[2] `http://www.cisl.ucar.edu/css/software/mudpack`

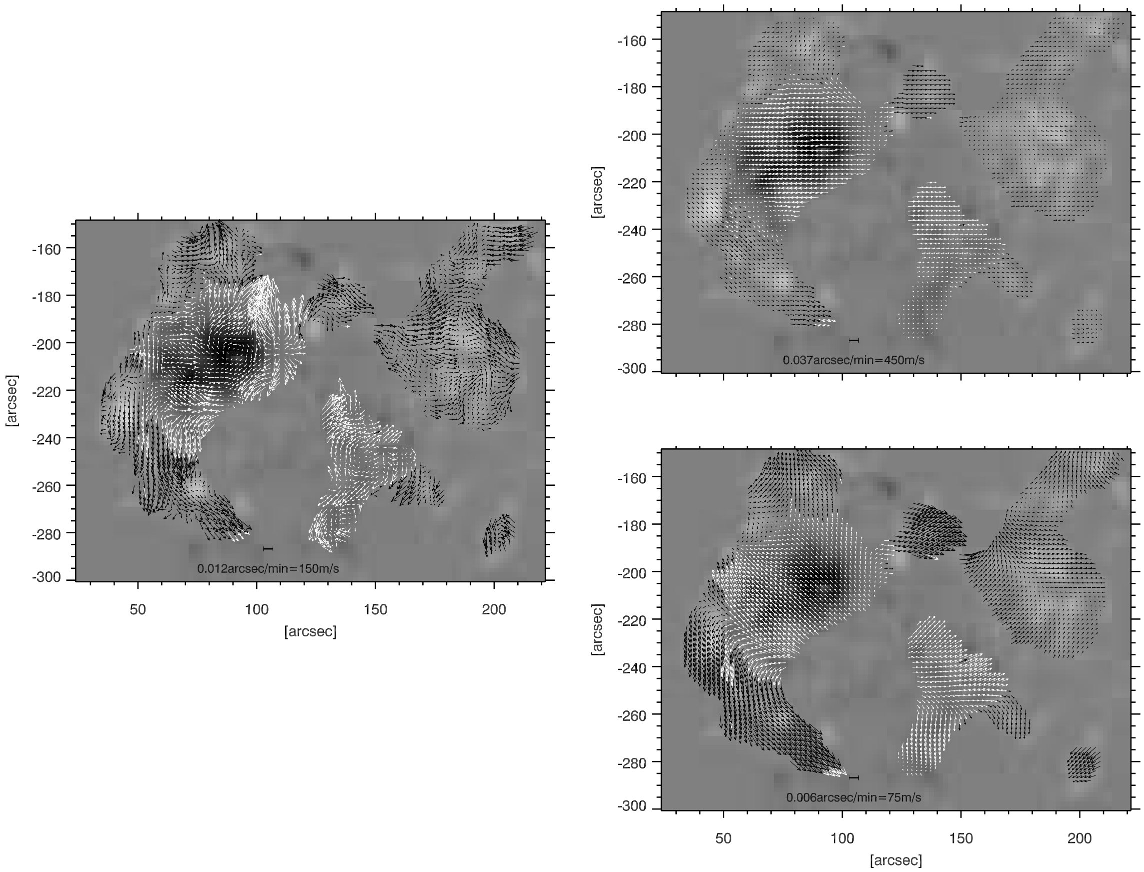

Figure 2: Magnetic footpoint velocity field for AR8210 at 19:24 UT on 1998 May 1 determined from the DAVE (left) and LCT (right). Frame separations of $\Delta t = 8$ min (top right) and $\Delta t = 4$ hours and 16 min (bottom right).

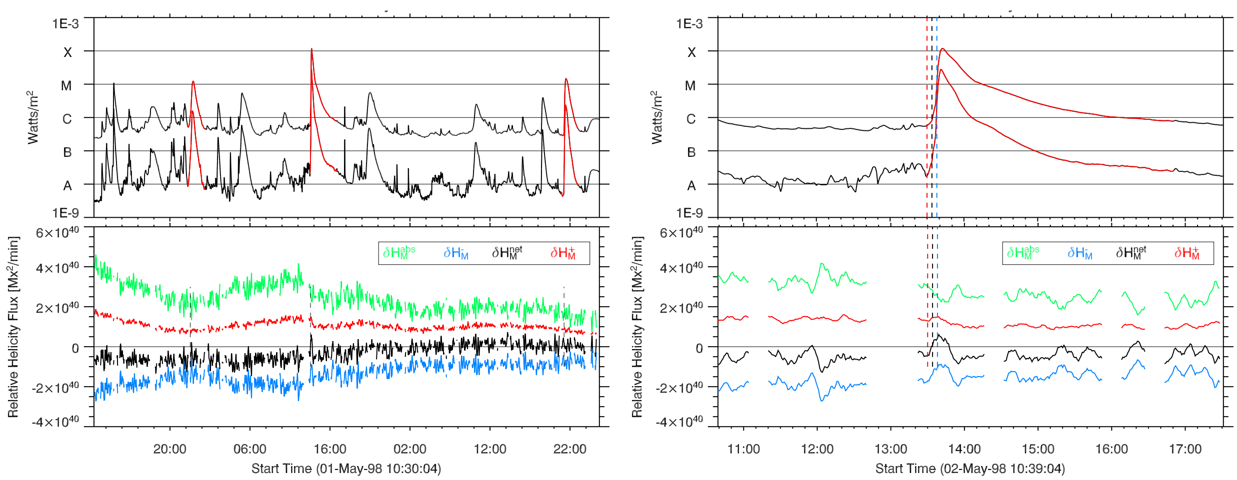

Figure 3: Helicity flux and GOES soft-xray flux for AR8210.

The helicity flux calculations indicate that the net helicity flux $\delta H_{\rm M}^{\rm net} = H_{\rm M}^{+} + H_{\rm M}^{-}$, where $H_{\rm M}^{\pm}$ is the helicity flux of the $\pm$ footpoints, is negative prior to the flare around 14:00 UT at which time the net helicity flux becomes positive. The peak in helicity flux concomitant with the flare is likely caused by line profile distortion during the flare. However, the strong change in $\delta H_{\rm M}^{\rm net} = \left|H_{\rm M}^{+}\right| + \left|H_{\rm M}^{-}\right|$ during the rise of the flare is likely an indication of a *permanent* change in the orientation of the magnetic field.

C. *Benchmark **DAVE** and flux codes against MHD simulations:* $\boldsymbol{u}_{\mathrm{F}}$ *based on known* $\boldsymbol{v}_t$ *and* v_n *and* $\boldsymbol{B}$*.* **Progress:** Extensive benchmarks have been carried out for DAVE against the analastic high-β MHD code ANMHD and documented in a peer-reviewed journal article under review (Welsch et al., 2007). DAVE performed well in comparison with LCT, Inductive Local Correlation Tracking (ILCT) (Welsch et al., 2004), and Minimum Energy Fit (MEF) (Longcope, 2004).

OUTLOOK FOR YEAR 2

A. *Extend the **DAVE** algorithm to implement all components of Vector Magnetogram data: **DAVE-VM**.* **Initial Progress:** We have already made some preliminary progress towards including vector magnetogram data and we are planning to extend the scope of this work to include line-of-sight Doppler velocities.

B. *Develop tool for accurately evolving* $\boldsymbol{B}$ *in a prescribed flow according to vector induction equation and benchmark **DAVE-VM** against it.*
Work In Progress.

C. *Identify important solar events with vector magnetogram coverage for magnetogram study.*
Work In Progress.

REFERENCES

Beck, J. G. 2000, Sol. Phys., 191, 47

Chae, J., Jeong, H., & Lim, E. 2006, in COSPAR, Plenary Meeting, Vol. 36, 36th COSPAR Scientific Assembly, 880–+

Fisher, G. H., & Solar MURI Team. 2003, AAS/Solar Physics Division Meeting, 34

Georgoulis, M. K., & LaBonte, B. J. 2006, ApJ, 636, 475

Gudiksen, B. V., & Nordlund, Å. 2002, ApJ, 572, L113

Howard, R. F., Harvey, J. W., & Forgach, S. 1990, Sol. Phys., 130, 295

Huang, D.-Y. W. G. L., & Falthammar, C. G. 2002, Astrophys. Space Sci., 282, 421

Javaraiah, J. 1999, Sol. Phys., 189, 289

Longcope, D. W. 2004, ApJ, 612, 1181

Pohjolainen, S., Maia, D., Pick, M., Vilmer, N., Khan, J. I., Otruba, W., Warmuth, A., Benz, A., Alissandrakis, C., & Thompson, B. J. 2001, ApJ, 556, 421

Riley, P., Linker, J. A., & Mikić, Z. 2001, J. Geophys. Res., 106, 15889

Roussev, I. I., Gombosi, T. I., Sokolov, I. V., Velli, M., Manchester, W., DeZeeuw, D. L., Liewer, P., Tóth, G., & Luhmann, J. 2003, ApJ, 595, L57

Scherrer, P. H., Bogart, R. S., Bush, R. I., Hoeksema, J. T., Kosovichev, A. G., Schou, J., Rosenberg, W., Springer, L., Tarbell, T. D., Title, A., Wolfson, C. J., Zayer, I., & MDI Engineering Team. 1995, Sol. Phys., 162, 129

Schuck, P. W. 2006, ApJ, 646, 1358, http://www.journals.uchicago.edu/cgi-bin/resolve?id=doi:10.1086/505015

Sterling, A. C., & Moore, R. L. 2001, ApJ, 560, 1045

Sterling, A. C., Moore, R. L., Qiu, J., & Wang, H. 2001, ApJ, 561, 1116

Ward, F. 1965, ApJ, 141, 534

Warmuth, A., Hanslmeier, A., Messerotti, M., Cacciani, A., Moretti, P. F., & Otruba, W. 2000, Sol. Phys., 194, 103

Welsch, B. T., Abbett, W. P., DeRosa, M. L., Fisher, G. H., Georgoulis, M. K., Kusano, K., Longcope, D. W., Ravindra, B., & Schuck, P. W. 2007, ApJ, under review: http://solarmuri.ssl.berkeley.edu/~welsch/public/manuscripts/Shootout/R%evision/ms.pdf

Welsch, B. T., Fisher, G. H., & Abbett, W. P. 2004, ApJ, 620, 1148, http://solarmuri.ssl.berkeley.edu/~welsch/public/software

Xia, Z.-G., Wang, M., Zhang, B.-R., & Yang, Y.-H. 2002, Chinese Astronomy and Astrophysics, 26, 164